Liquid Lens Module with Wide Field-of-View and Variable Focal Length

Sang Won Seo,[1] Seungoh Han,[2,*] Jun Ho Seo,[1] Woo Bum Choi,[3] and Man Young Sung[1]

[1]Dept. of Electrical Engineering, Korea University, Anam-dong, Seongbuk-gu, Seoul 136-701, Korea
[2]Research Center for Convergence Technology, Hoseo University, Asan-si, Chungnam 336-795, Korea
[3]BNP Science Co. Ltd.

A novel wide angle and variable-focus imaging module based on a miniaturized liquid lens is presented for capsule endoscopy applications. For these applications, it is desirable to have features such as a wide field of view (FOV), variable focus, small size, and low power consumption, thereby taking full advantage of the miniaturized liquid lens. The proposed imaging module has three aspheric plastic lenses for a wide FOV, and one liquid lens that can change the focal length by as much as 24.5 cm with a bias voltage difference of 23 V_{rms} for variable focusing. The assembled lens module has an overall length of 8.4 mm and a FOV of 120.5°. The realized imaging module including the proposed lenses is small enough to be inserted into a capsule endoscope, and it is expected to improve the diagnostic capability of capsule endoscopes.

Keywords: MEMS, liquid lens, wide angle, variable focus, capsule endoscope

1. INTRODUCTION

Capsule endoscopes have been increasingly accepted in medical diagnostics during the past few years.[1,2] Despite the recent technical advances such as real-time viewing[1] and back-and-forth movement,[3] optical improvements such as auto-focusing and zooming are still needed. When a capsule endoscope captures images of the intestinal wall, it is generally too close to the wall. Therefore, an imaging module for a capsule endoscope must have a wide field of view (FOV) to cover a wider region of the intestinal wall. Also, there are some portions of the intestine where the endoscope cannot take images because it moves intermittently due to the peristaltic motion of the intestine. Thus, a variable-focus capability is also desirable.

Since the power consumption and size are the key limitations in a capsule endoscope, micro-electromechanical system (MEMS) technology can be an appropriate solution due to its small size and low power consumption.[4-5] MEMS-based liquid lenses have attracted increasing attention for digital imaging applications due to their small size, light weight, low power consumption, and low cost.[6-8] Most MEMS lenses are developed for the consumer electronics industry, but there is also an effort to use liquid lens as the next-generation zoom lens without motorized moving parts.[9]

This paper presents a wide angle and variable-focus imaging module based on a miniaturized liquid lens for capsule endoscopy applications. The lens module consists of three aspheric plastic lenses for a wide FOV, and one variable-focus liquid lens to minimize volume, considering the limited space inside a capsule endoscope. A liquid lens based on MEMS technology was prepared and then the aspheric lenses were designed and fabricated. Finally, the lens module was assembled and tested by capturing test images with the assembled module.

2. LIQUID LENS FOR VARIABLE-FOCUS OPERATION

Liquid lenses operate based on the electrowetting phenomenon.[10] The electrowetting phenomenon, based on electrocapillary behavior, is a contact angle change in the conducting liquid when an electric potential is applied between the conducting liquid and a counter electrode. Due to the thin dielectric layer between the conducting liquid and the counter electrode, the system can be modeled as a capacitor, and the modified contact angle θ from the initial contact angle θ_0 can be calculated as a function of the applied voltage bias V using the Young-Lippmann equation[11]:

$$\gamma_{LV}[\cos\theta - \cos\theta_0] = \frac{1}{2}\frac{\varepsilon_0\varepsilon_r}{d}V^2 \qquad (1)$$

where γ is the surface tension, d is the thickness of the dielectric layer, and the subscripts L and V indicate the (conducting) liquid and (surrounding) vapor, respectively. ε_0 and ε_r are the dielectric constant of the free space and the relative dielectric constant of the dielectric material, respectively.

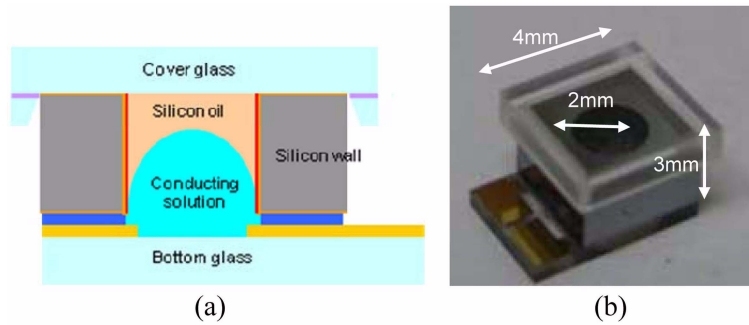*Corresponding author: sohan@hoseo.edu

Fig. 1. (a) Cross-sectional view of the liquid lens and (b) the photograph of the fabricated liquid lens.
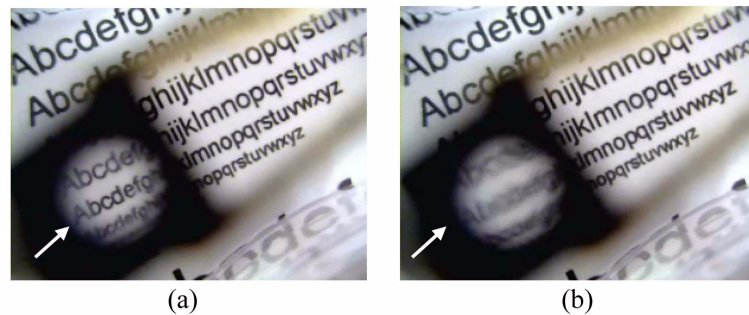

Fig. 2. Focal length variation due to the applied voltage: (a) with the flat interface and (b) with the curved interface between the conducting liquid and the silicon oil.

Figure 1 shows a cross sectional view of the proposed liquid lens and a photograph of the fabricated lens. The liquid lens consists of three parts: a cover glass, a cylinder liquid chamber, and a bottom glass. The liquid chamber consists of a silicon wafer with a thickness of 525 μm, wherein the silicon wall itself acts as the counter solid electrode. The cylinder has a vertical sidewall and is 2 mm in diameter. To form the vertical sidewall, a laser hole process is used rather than anisotropic wet etching. After the laser hole processing, the dielectric layer was deposited and this was followed by a Teflon layer coating for the hydrophobic surface. The other electrode was fabricated on the bottom glass wafer, which is partially coated with dry film photoresist (DFR). Through the open window in the DFR, the conducting liquid was electrically connected to bottom electrode. The prepared liquid chamber and the bottom glass were then assembled and bonded together. Before sealing the liquid lens with the cover glass, a conducting liquid of 5 wt. % NaOH and silicon oil were injected into the silicon chamber. The fabricated device has a size of 4 mm × 4 mm × 3 mm with an optical hole diameter of 2 mm.[12]

To verify the contact angle change due to the applied electric bias, the fabricated liquid lens was tested as shown in Fig. 2. The alphabet was read through the liquid lens at different bias conditions. With a flat interface between the conducting liquid and silicon oil, the alphabet was seen clearly through the liquid lens as shown in Fig. 2(a). By changing the voltage bias, the contact angle of the liquid lens was

changed, and therefore the alphabet became blurred as shown in Fig. 2(b). Also, the leakage current of the fabricated liquid lens was measured to be less than 1 nA, which demonstrated that the liquid lens consumed little electric power.

3. LENS MODULE ASSEMBLY AND TEST

Since three aspheric lenses will be coupled with the variable-focus liquid lens, the overall lens should be designed considering of the focal length variation of the liquid lens. Including the effective focal lengths, the design parameters and performance of the total lens module are summarized and presented in Table 1 where the minimum and maximum

Table 1. Specifications of the designed lens module

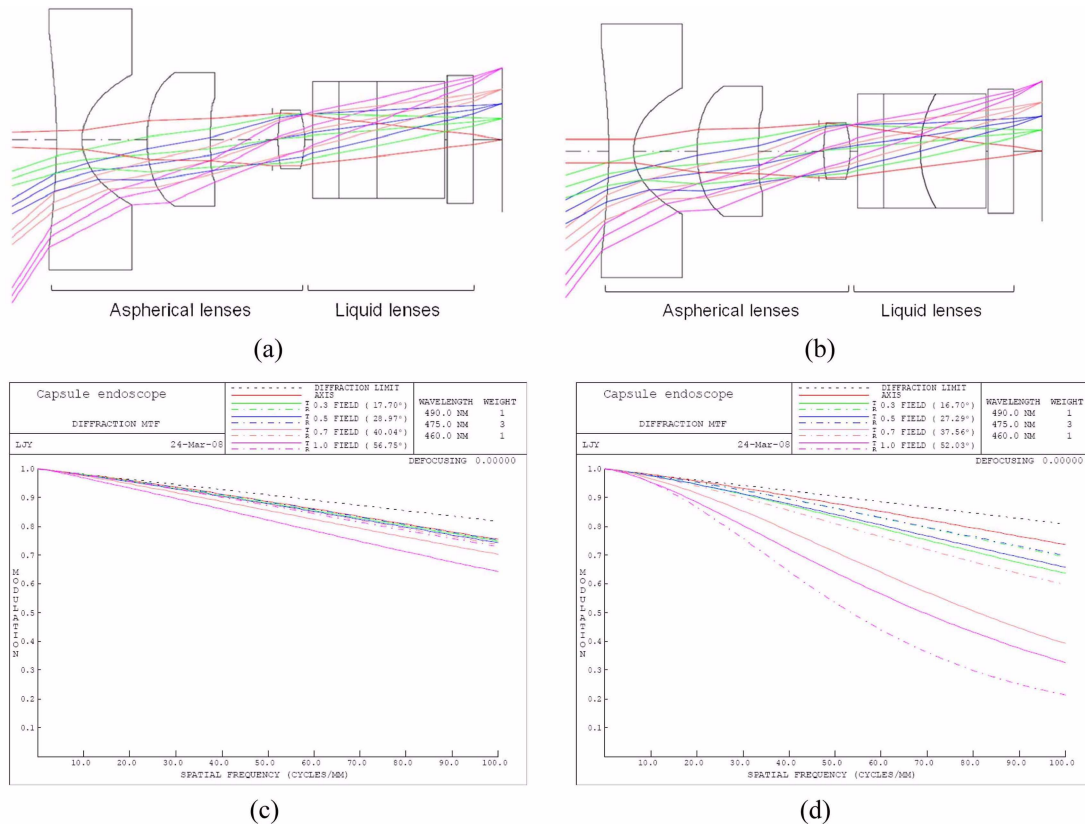| Max. image height		ϕ2.57 mm
F/NO.		3.0
FOV		107° at 5 mm image 104° at 200 mm image
Effective focal length		1.19 mm at 5 mm image 1.35 mm at 200 mm image
MTF (image height = ϕ2.57mm)	0.0 Field	75.6%
	0.5 Field	R 75.3% / T 74.3%
	0.7 Field	R 73.4% / T 70.1%
Relative illumination		55.2% at 5 mm image
OAL		8.4 mm

(a)

(b)

(c)

(d)

Fig. 3. Design of the wide-angle, variable-focus lens module: (a) ray trace for the 5mm image distance, (b) ray trace for the 20 mm image distance, (c) MTF for the 5 mm image distance, and (d) MTF for the 20 mm image distance.
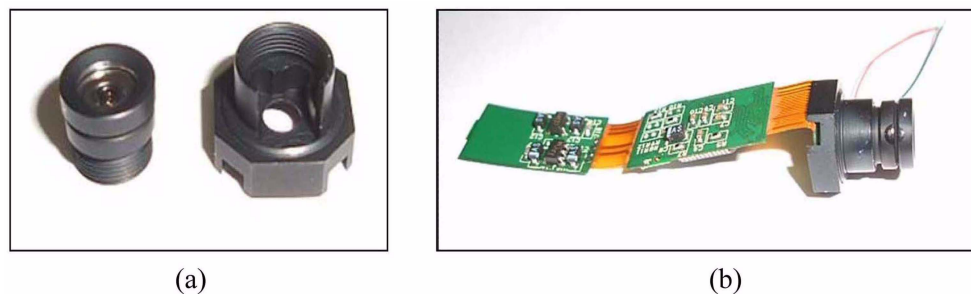

(a)

(b)

Fig. 4. The fabricated lens module: (a) aspherical lens module, (b) assembled lens module.

distances to the object are assumed to be 5 mm and 200 mm, respectively. The lens module was designed as shown in Fig. 3. The three aspheric lenses are located at the front in the lens module, followed by the liquid lens. The image sensor was assumed to have a 324 × 324 pixel array, and the size of each pixel is 5.6 μm.

The designed lens module was fabricated and assembled as shown in Fig. 4. Figure 5 shows the image captured with the fabricated lens module. When an external bias of 31 V_{rms} was applied, the width of the captured object was 35 mm while the distance between the lens module and the object was 10 mm; from this, the FOV was calculated to be 120.5°C.
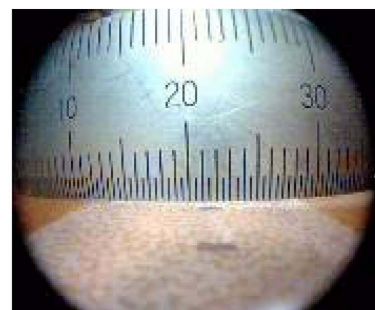

Fig. 5. The wide FOV: image taken with the fabricated lens module at the bias voltage of 31V_{rms}.
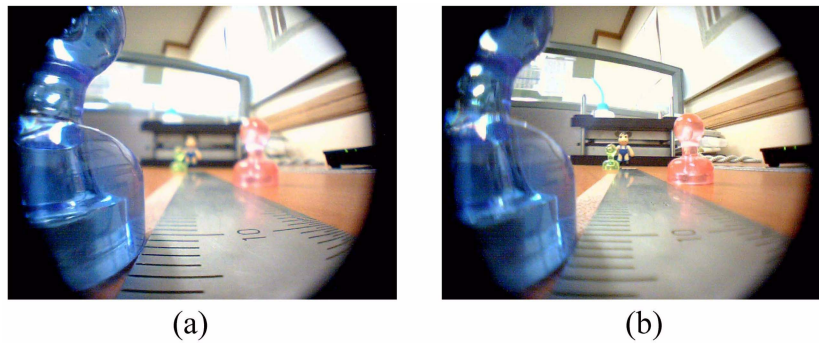
$$(a) \hspace{6cm} (b)$$

Fig. 6. Images taken with the fabricated imaging module: (a) With the applied bias voltage of 34 V_{rms} and (b) With the applied bias voltage of 11 V_{rms}.

When a bias voltage of 34 V_{rms} was applied to the liquid lens, the curvature of the liquid interface was flattened resulting in the object close to the lens module being captured clearly. As the bias voltage was decreased to 11 V_{rms}, the curvature of the liquid lens reached its maximum, and therefore the lens module focused on an object located at 250 mm from the imaging module. All corresponding images from the charge-coupled device (CCD) image sensor are shown in Fig. 6. That is, Fig. 6(a) shows the image when an external bias of 34 V_{rms} was applied and where the object in focus was 5 mm from the lens module. Figure 6(b) shows the image with an applied voltage bias of 11 V_{rms}.

The maximum driving voltage to control the focal length of the lens module was 34 V_{rms}, which cannot be supplied directly from the battery generally used in capsule endoscopes. However, the required driving voltage can be provided if a single additional converter chip is included.

4. CONCLUSION

This paper presents a novel imaging lens module for capsule endoscopy applications which has a wide FOV and variable focusing. Since a capsule endoscope must be small and have low power consumption, the proposed imaging module adopts a MEMS-based liquid lens for variable focusing. Three aspheric lenses were added for a wide FOV of 120.5° and a focal length change of 24.5 cm was measured with a bias voltage difference of 23 V_{rms}(= 34 V_{rms} − 11 V_{rms}). The developed imaging lens module provides a new realizable approach to capsule endoscopes in terms of optical improvements.

REFERENCES

1. R. Sidhu, D. S. Sanders, and M. E. McAlindon, *Brit. Med. J.* **332**, 528 (2006).
2. O.-Y. Mang, S.-W. Huang, Y.-L. Chen, H.-H. Lee, and P.-K. Weng, *Opt. Eng.* **46**, 103002 (2007).
3. B. Kim, S. Lee, J. H. Park, and J.-O. Park, *Proc. Int. Conf. Robotics and Biomimetics*, p. 22 (2004).
4. S. P. Lee, *Elec. Mater. Lett.* **6**, 7 (2010).
5. S.-H. Yi, H. Cho, and S. Han, *Elec. Mater. Lett.* **5**, 55 (2009).
6. F. Krogmann, W. Mönch, and H. Zappe, *J. Opt. A: Pure Appl. Opt.* **8**, 330 (2006).
7. S. Kuiper and B. H. W. Hendriks, *Appl. Phys. Lett.* **85**, 1128 (2004).
8. B. Berge, *Proc. IEEE MEMS*, p. 3 (2005).
9. R. Peng, J. Chen, C. Zhu, and S. Zhuang, *Opt. Express* **15**, 6664 (2007).
10. F. Mugele and J. C. Baret, *J. Phys. Condes. Matter.* **17**, 705 (2005).
11. H. J. J. Verheijen and M. W. J. Prins, *Langmuir* **15**, 6616 (1999).
12. S. W. Seo, S. Han, J. H. Seo, Y. M. Kim, M. S. Kang, N. G. Min, W. B. Choi, and M. Y. Sung, *Jpn. J. Appl. Phys.* **48**, 052404 (2009).